prone to autoimmunity, expansion of autoreactive TCR Vβ domains occurs after early postnatal thymectomy[24]. In the model system described here, $CD4^+$ $V\beta6^+$ cells decrease with age in peripheral lymphoid tissues of neonatal BALB.D2.Mls^a mice[14], and early postnatal thymectomy (performed after 3 or 6 days) does not result in a significantly increased proportion of $CD4^+$ $V\beta6^+$ cells in adult animals (data not shown). The data described here therefore indicate that the expansion of potentially autoreactive T cells seen in autoimmune strains after neonatal thymectomy could depend on additional genetic factors (perhaps controlling the effective presentation of autoantigens). In strains where such clonal expansion does not occur (such as BALB.D2.Mls^a), it is nevertheless not clear whether the small proportion of residual $CD4^+$ $V\beta6^+$ cells in the periphery represents an anergic population or alternatively a small subset of $V\beta6^+$ cells that has escaped clonal deletion because of lack of reactivity to Mls-1^a antigens. □

Received 19 October; accepted 19 December 1989.

1. Kappler, J. W., Roehm, N. & Marrack, P. *Cell* **49,** 263-271 (1987).
2. Wyllie, A. H., Morris, R. G., Smith, A. L. & Dunlop, D. *J. Path.* **142,** 67-77 (1984).
3. Cohen, J. J. & Duke, R. C. *J. Immun.* **132,** 38-42 (1984).
4. Kappler, J. W., Staerz, U., White, J. & Marrack, P. *Nature* **332,** 35-40 (1988).
5. MacDonald, H. R. *et al. Nature* **332,** 40-45 (1988).
6. Pullen, A. M., Marrack, P. & Kappler, J. W. *Nature* **335,** 796-801 (1988).
7. Fry, A. M. & Matis, L. A. *Nature* **335,** 830-832 (1988).
8. Tomonari, K. & Lovering, E. *Immunogenetics* **28,** 445-451 (1988).
9. Bill, J., Kanagawa, O., Woodland, D. L. & Palmer, E. *J. exp. Med.* **169,** 1405-1419 (1989).
10. Kanagawa, O., Palmer, E. & Bill, J. *Cell Immun.* **119,** 412-426 (1989).
11. Fowlkes, B. J., Schwartz, R. H. & Pardoll, D. M. *Nature* **334,** 620-623 (1988).
12. MacDonald, H. R., Hengartner, H. & Pedrazzini, T. *Nature* **335,** 174-176 (1988).
13. Kisielow, P., Bluthmann, H., Staerz, U. D., Steinmetz, M. & von Boehmer, H. *Nature* **333,** 742-746 (1988).
14. Schneider, R. *et al. J. exp. Med.* **169,** 2149-2158 (1989).
15. Wyllie, A. H., Kerr, J. F. R. & Currie, A. R. *Int. Rev. Cytol.* **68,** 251-305 (1980).
16. Shi, Y., Sahai, B. M. & Green, D. R. *Nature* **339,** 625-626 (1989).
17. Smith, C. A., Williams, G. T., Kingston, R., Jenkinson, E. J. & Owen, J. J. T. *Nature* **337,** 181-184 (1989).
18. Russell, J. H. *Immunol. Rev.* **72,** 97-118 (1983).
19. McConkey, D. J. *et al. Archs Biochem. Biophys.* **269,** 365-370 (1989).
20. McConkey, D. J., Hartzell, P., Nicotera, P. & Orrenius, S. *FASEB J.* **3,** 1843-1849 (1989).
21. Ceredig, R., Dialynas, D. P., Fitch, F. W. & MacDonald, H. R. *J. exp. Med.* **158,** 1654-1671 (1983).
22. Qin, S., Cobbold, S., Benjamin, R. & Waldmann, H. *J. exp. Med.* **169,** 779-794 (1989).
23. Rammensee, H.-G., Kroschewski, R. & Frangoulis, B. *Nature* **339,** 541-544 (1989).
24. Smith, H., Chen, I.-M., Kubo, R. & Tung, K. S. K. *Science* **245,** 749-752 (1989).
25. Festenstein, H. & Berumen, L. *Transplantation* **37,** 322-324 (1984).
26. Payne, J. *et al. Proc. natn. Acad. Sci. U.S.A.* **85,** 7695-7698 (1988).
27. Haskins, K. *et al. J. exp. Med.* **160,** 452-471 (1984).
28. Pierres, A. *et al. J. Immun.* **132,** 2775-2782 (1984).
29. MacDonald, H. R. & Zaech, P. *Cytometry* **3,** 55-58 (1982).

ACKNOWLEDGEMENTS. We thank P. Zaech and C. Knabenhans for flow cytometry and A. Zoppi for preparation of the manuscript. We also acknowledge the contribution of R. Schneider and H. Hengartner (Institute for Pathology, University Hospital, Zurich) to the initial stages of this work.

A dimension reduction framework for understanding cortical maps

Richard Durbin* & Graeme Mitchison†

* Department of Psychology, Stanford University, California 94305, USA
† Physiological Laboratory, Downing Street, Cambridge CB2 3EG, UK, and The Research Centre, King's College, Cambridge CB2 1ST, UK

We argue that cortical maps, such as those for ocular dominance, orientation and retinotopic position in primary visual cortex[1], can be understood in terms of dimension-reducing mappings from many-dimensional parameter spaces to the surface of the cortex. The goal of these mappings is to preserve as far as possible neighbourhood relations in parameter space so that local computations in parameter space can be performed locally in the cortex. We have found that, in a simple case[2], certain self-organizing models[3,4] generate maps that are near-optimally local, in the sense that they come close to minimizing the neuronal wiring required for local operations. When these self-organizing models are applied to the task of simultaneously mapping retinotopic position and orientation, they produce maps with orientation vortices resembling those produced in primary visual cortex[5]. This approach also yields a new prediction, which is that the mapping of position in visual cortex will be distorted in the orientation fracture zones[5].

In addition to the retinotopic map in primary visual cortex (V1), orientation selectivity and ocular dominance are mapped in patterns of stripes or patches[1], as has been strikingly demonstrated by recent work[5] using voltage-sensitive dyes (Fig. 2*a*). A characteristic feature of all these mappings is that they are smooth, that is, neighbouring cells on the cortex have similar response properties. Because receptive field properties are columnar, that is, are similar in a penetration normal to the cortical surface[6], the cortex can be considered as a two-dimensional (2-D) sheet on which response properties are mapped. We assume that there are cells in V1 that are responsive to stimuli of each orientation in each eye at each position in visual space. We should therefore envisage a parameter space of response properties whose dimensions are orientation, ocular dominance and retinotopic position, which is mapped onto the cortical sheet. A similar organization, in which several response properties are all smoothly mapped into one area, is seen in other cortical areas[7,8].

The smoothness of cortical maps tells us that neighbouring points on the cortex correspond to nearby points in parameter space. But we propose here, following the arguments of Cowey[9], that the main principle of cortical mapping operates the other way around, that is, neighbouring points in parameter space should map close together on the cortex. The underlying assumption is that most operations performed in the cortex are local, in the sense that they involve neighbouring parameter values. The construction of inhibitory surrounds and the sharpening of orientation tuning[10] are examples of this. Such operations require connections between neurons in the cortex that represent similar parameter values. Here we use the length of cortical wiring needed to connect these neurons as a measure of how locally the computation is performed on the cortex. Minimizing wire length will ensure that cells representing similar parameter values lie close together. This approach is not restricted to V1. In general, it can be argued that those properties that are mapped in a given cortical area are precisely those that will be involved in local computational interactions, such as the sharpening of receptive field characteristics or extraction of new properties.

The parameter space will generally be of higher dimension than the 2-D cortical sheet. Thus in V1 there are at least four dimensions: two of retinotopic space, one of orientation and one of ocular dominance. Because of the reduction in dimension in mapping from parameter space to cortex, the requirement that all neighbouring points in parameter space should be neighbours on the cortex cannot be met. What is the best that can be achieved?

We have previously studied this problem[2] in a highly simplified setting where a 2-D discrete parameter space ($N \times N$) is mapped onto a 1-D 'cortex'. The way we formulated this problem and typical results are shown in Fig. 1. Our main conclusion is that optimal dimension reduction mappings show many of the features of cortical maps, but only if the mapping cost is calculated using a nonlinear function of wire length that favours many short connections while allowing a few long ones. The basic properties that the simplified model predicts are that the maps on the cortex are smooth, and that both parameters show jitter to accomodate mapping of the other parameter.

Unfortunately, it is computationally unfeasible to extend this kind of minimization procedure to higher-dimensional mappings to obtain optimal mappings on a 2-D model cortex. But this might not have been profitable anyway; we cannot claim to have an accurate measure of biological cost, nor is it likely that an explicit cost minimization process occurs during cortical development. Our strategy was therefore to examine self-organizing algorithms as models for the development of cortical maps. These have a much better claim to biological plausibility, and we show below that the maps they produce can achieve a

low cost by our wiring criterion, and that they can also generate maps of orientation like those seen in V1.

The basic assumption of these models, which has much support from sensory physiology[11-14], is that neurons develop their receptive-field characteristics under the influence of incoming neural activity. The rules for adjusting the response properties of cortical units are (1) that there are competitive interactions between units that correspond to any given input, after which those units that fire most strongly become more responsive to the input, and (2) that units also strengthen their responses to inputs that their neighbours respond to. The first rule leads to a competitive sharing-out of the domain of inputs among units, while the second rule imposes a continuity constraint leading to the development of a coherent map. Such algorithms have been able to account for many of the phenomena of plasticity of neural maps. The details of the algorithm we use are given in the legend to Fig. 2.

To what extent does this self-organizing procedure minimize wire length? If we apply our algorithm to the simplified problem described above (2-D parameter space to 1-D cortex), we obtain

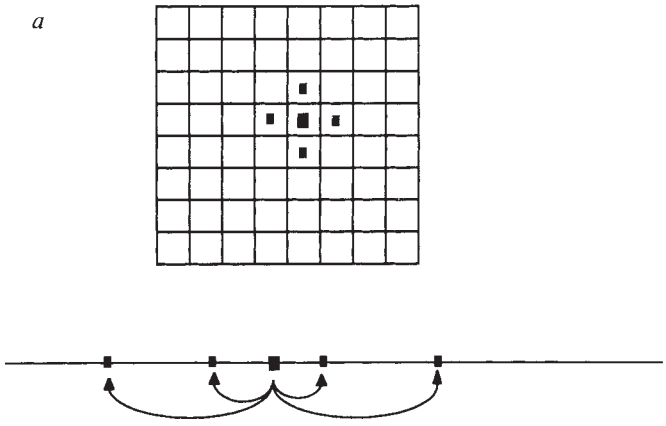

FIG. 1 *a*, Simplified model for dimension reduction. Points in the $N \times N$ grid are mapped to the line cortex by the function f. A point (large dot) and its four neighbours (small dots) are shown in the grid, and their images under f are shown on the line below. The 'wire length' for the mapping is the sum of the absolute values of differences between images of adjacent points, raised to the power p (L_p metric). Thus the link between $f(i, j)$ and $f(i, j+1)$ contributes $|f(i, j) - f(i, j+1)|^p$ to the cost. If $p > 1$, then this penalizes long-distance costs heavily, whereas if $p < 1$, it places an emphasis on mapping as many neighbours as close as possible, while allowing a few longer connections. The dependence of the optimal mapping on p is discussed in detail in ref. 2. *b*, Mapping found by applying our cost-minimizing algorithm to a 10×10 array with $p = 1$. The algorithm works by a structured search process involving generation and selection of random variants (4×10^7 operations in total). The mapping is depicted by showing the value of f (the integer within each circle) at each grid location. To allow the sequence of numbers to be followed more easily, lines have been drawn between locations with adjacent values. The mapping shown here can be proved to be optimal[2], with cost 914. The main characteristic of the mapping, shown clearly in the middle region, is that as the integers are run through (equivalent to moving along the cortex), the values of one parameter are rapidly cycled through with regular jumps, whereas the other advances one notch at a time. This is unlike cortical maps, which change more continuously, although with some random scatter. *c*, Mapping found by applying the cost-minimizing algorithm described above, minimizing with $p = \frac{1}{2}$. The organization is typical of mappings obtained when $p < 1$ (ref. 2). The cost is 335.8. This mapping has the fine-scale cortical properties that were lacking in *b*: smoothness (neighbouring numbers are nearby in the grid), and more equal treatment of the two parameters. *d*, Mapping found by applying the self-organizing algorithm (see legend to Fig. 2*b*). The cost ($p = \frac{1}{2}$) is 347.1. This is close to that for the optimized mapping shown in *c*, and many of the general features of the mapping in *c* are also seen here. For comparison, the cost of the mapping in *b* with $p = \frac{1}{2}$ is 352.3. Although for a 10×10 array the costs of *b* and *d* are close, the difference will increase with N, because the cost of *b* scales as $N^{2.5}$, whereas that for the more folded structures of *c* and *d* is expected to scale as $N^2 \log N$.

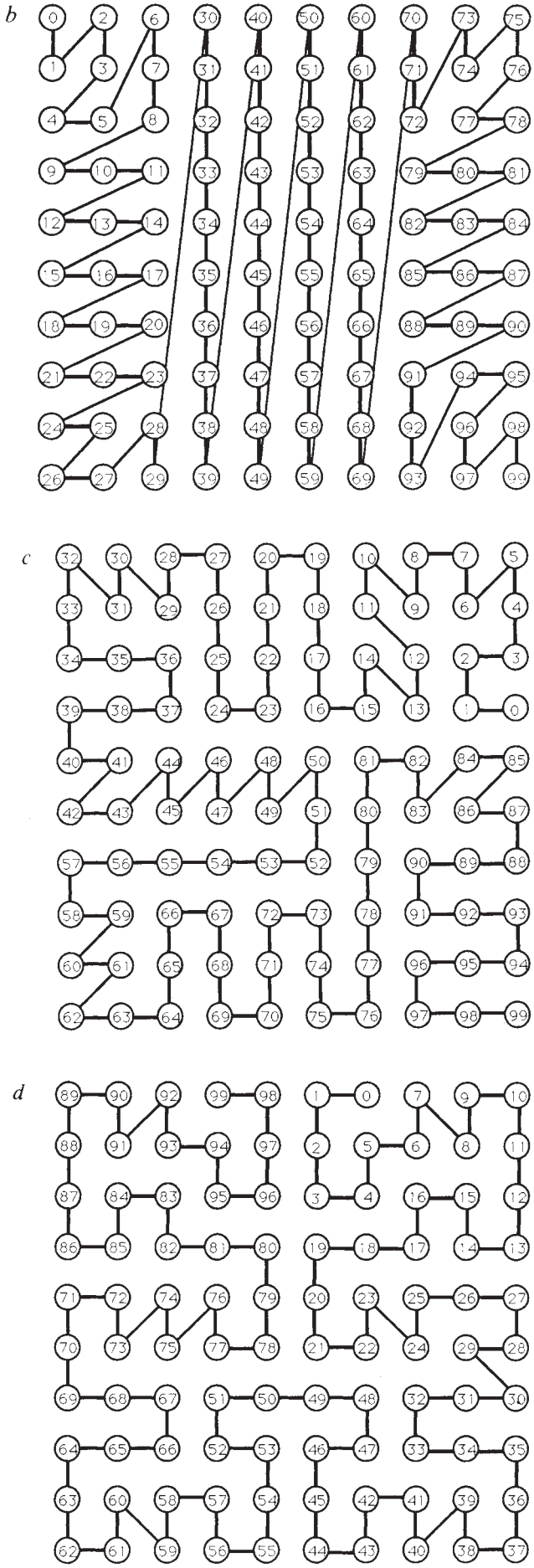

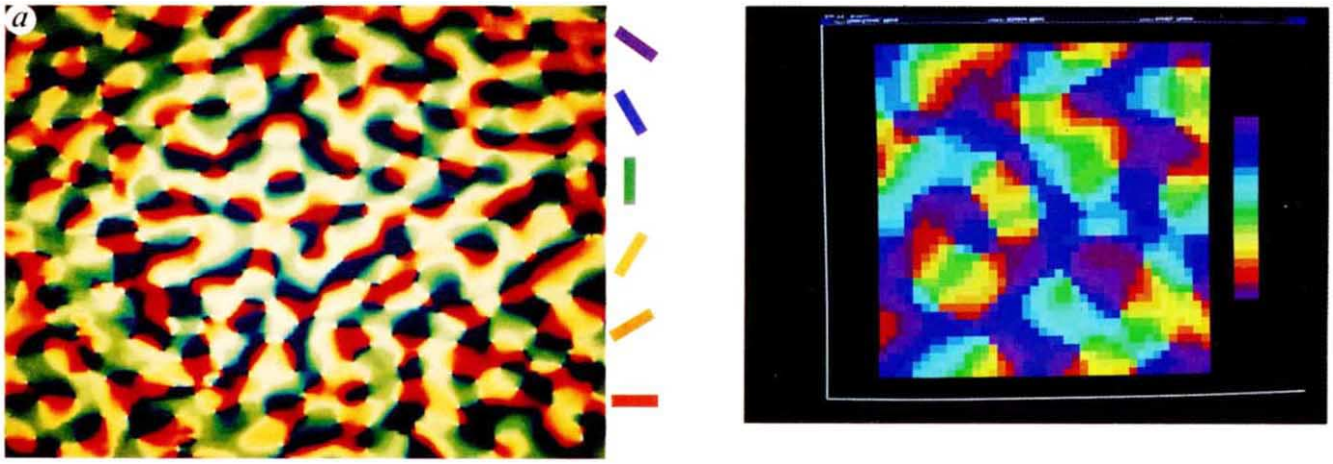

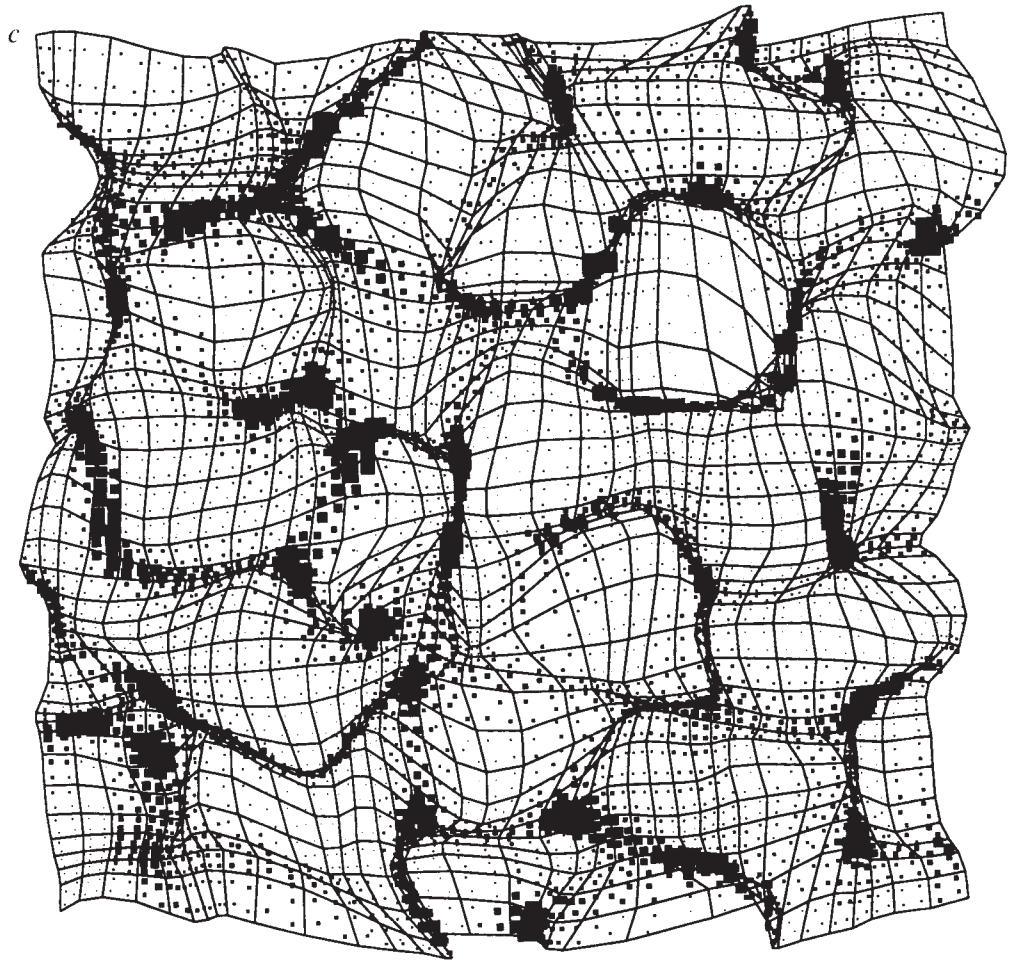

FIG. 2 *a*, Colour-coded representation of orientation in macaque striate cortex, derived by using voltage-sensitive dyes (from ref. 5). The bars indicate the range of orientations associated with each colour. The horizontal width of the image corresponds to 8 mm on the cortical surface. A prominent feature is the regular occurrence of singularities, or points in whose vicinity all orientations are present. *b* and *c*, Results of a simulation of an elastic net self-organizing model[3] for the joint development of orientation specificity and retinotopy. We considered a 40×40 array of cortical units, each of whose receptive fields are parameterized by a 4-D vector $\mathbf{y}_j = (x, y, r, \theta)$, where x, y is the centre of the receptive field in visual space, and the polar coordinates (r, θ) encode preferred orientation $\theta/2$ (we divide by 2 because direction is not mapped in V1[17]) and degree of orientation tuning r. Computationally, r and θ were treated in their cartesian forms $\eta = r\cos\theta$, $\chi = r\sin\theta$. We used periodic boundary conditions in x, y to remove edge effects. Random stimuli $\mathbf{x}$ were drawn from the same 4-D space, with (x, y) uniform in $[0, 1]$, θ uniform in $[0, \pi/2]$, $r = 0.17$. Even when visual input is absent, as during the development of orientation selectivity in monkey cortex[18], local orientated patterns of neural activity can be assumed[19,20]. For each stimulus, the activity levels of the cortical units were calculated using gaussian receptive fields, then normalized: $W_j = \exp(-(\mathbf{x}-\mathbf{y}_j)^2/2K^2)$, $w_j = W_j/\Sigma W_k$. Receptive fields of all units j were then updated according to $\Delta\mathbf{y}_j = \alpha w_j(\mathbf{x}-\mathbf{y}_j) + \beta \sum_{k\in N}(\mathbf{y}_k - \mathbf{y}_j)$, where k in the sum ranges over the set N of direct neighbours to unit j in the cortical array. The first term in $\Delta\mathbf{y}_j$ is Hebbian. The second tends to make neighbours have similar receptive fields. Parameter values were $\alpha = 0.4$, $\beta = 0.0001$, $K = 0.06$. In fact, for reasons of computational efficiency, three sets of 216 random stimuli were used, and for each set a Gauss–Seidel procedure was used to rapidly find the stable configuration corresponding to repeated selection in the above procedure of the stimuli in the set. *b*, A colour-coded representation of the derived orientation map on the cortex. The magnification is about three times higher than in Fig. 2*a*. The strip shows the colours corresponding to a 180-degree cycle of orientations. *c*, A map in visual space showing simultaneously the distortion of the retinotopic map and the rate of change of orientation. The distorted grid represents the cortical array of cells. Each grid intersection is at the receptive field centre of the corresponding cell. The small filled squares show the rate of change of orientation at the corresponding point on the cortical map. The diameters of the squares are proportional to the sum of differences of orientation between a cell and a horizontal and vertical neighbour.

maps (for example, Fig. 1*d*) that look very like the computed minimal cost mapping (Fig. 1*c*). The costs of these maps are indeed close to minimal (Fig. 1 legend). It is surprising that the self-organizing models achieve such a low cost, because they actually operate in the opposite direction to our minimal wiring problem. They explicitly map from cortex to parameter space, assigning parameter values to cortical points, and attempting to put nearby cortical points close in parameter space. The goal of the wiring problem is to map from parameter space to cortex, putting nearby points in parameter space as close as possible on the cortex. In fact, the problem that the self-organizing models explicitly solve, that of finding smooth mappings from cortex to parameter space, is underconstrained—there are many such smooth mappings. The particular solutions that the models find are also good solutions to the wiring problem, because the way the mapping develops gives it a folded structure, which has the incidental effect of allowing many short connections between adjacent parameter values. We suggest, therefore, that self-organizing procedures could have evolved as a way of obtaining a satisfactory solution to the wiring problem at much less expense than a more direct minimization would require.

To help justify this claim, and the dimension reduction approach in general, we show below how a dimension-reducing self-organizing model predicts some of the observed features of cortical maps. Here we simulate the joint representation of retinal position and orientation selectivity, ignoring, for simplicity, ocular dominance and other V1 parameters, such as colour. We consider a 2-D cortex and a 4-D parameter space in which retinal position (2-D), orientation and orientation tuning (2-D) are represented. The map generated is shown in Fig. 2*b* and *c* (details of the procedures used are given in the legend to Fig. 2).

As can be seen, the orientation map (Fig. 2*b*) is qualitatively not unlike that found experimentally (Fig. 2*a*). We note that the map contains singularities like those seen in the data of Blasdel and Salama[5]. Figure 2*c* shows how retinal position is mapped; the cortex is depicted here as a grid mapped onto retinal space. Superposed on this grid are squares whose sizes represent the rate of change of orientation. We note that rapid orientation change is not confined to the singularities, but extends out to form bridges between them. This is roughly comparable to the 'fractures' described by Blasdel and Salama[5], although the rate of change is less in the stripes than at the singularities. Swindale has recently shown that his model for development of orientation selectivity[16] also gives rise to these features (personal communication). It therefore does not seem to be necessary to postulate a qualitative difference between the fracture zones and the domains. They could be a consequence of the developmental mechanism that gives rise to the orientation map.

A novel consequence of our approach is that because retinal space is treated as one of the parameter space variables, on the same footing as orientation, there are distortions in the retinotopic map. The most rapid changes of orientation tend to occur where retinal position changes most slowly (at the folds of the grid in Fig. 2*c*). From this it can be predicted that in the fracture zones, position will change slowly with more backtracking or jitter, whereas in the areas of more constant orientation selectivity, it will vary more smoothly and more rapidly. It will be interesting to see if systematic fine-scale mapping of retinotopy together with orientation supports this prediction. More generally, our approach indicates that wherever several parameters that are jointly involved in local computation are mapped, the fine structure of their mapping may be correlated. A previously observed example of this type of interaction is that orientation vortices tend to be positioned along the middle of ocular dominance stripes[5].

Our conclusion is that keeping connection lengths to a minimum could be an important goal of cortical map development, and that self-organizing algorithms could have evolved as mechanisms that are able to generate very good, although not perfect, solutions to this problem. We have shown here an example of how developmental models based on such self-organizing algorithms can have both explanatory and predictive power. □

Received 2 October; accepted 19 December 1989.

1. Hubel, D. H. & Wiesel, T. N. *Proc. R. Soc.* B **198,** 1–59 (1977).
2. Mitchison, G. J. & Durbin, R. M. SIAM *J. alg. disc. Meth.* **7,** 571–582 (1986).
3. Durbin, R. M. & Willshaw, D. *Nature* **326,** 689–691 (1987).
4. Kohonen, T. *Self-organization and Associative Memory* (Springer, Berlin, 1984).
5. Blasdel, G. G. & Salama, G. *Nature* **321,** 579–585 (1986).
6. Mountcastle, V. B. *J. Neurophysiol.* **20,** 408–434 (1957).
7. Kaas, J. H., Nelson, R. J., Sur, M. & Merzenich, M. M. in *The Organization of the Cerebral Cortex* (eds Schmitt, F. O., Worden, F. G., Adelman, G. & Denis, S. G.) 237–261 (MIT, Cambridge, Massachusetts, and London, 1981).
8. Suga, N. & O'Neill, W. E. *Science* **206,** 351–353 (1979).
9. Cowey, A. *Q. J. exp. Psychol.* **31,** 1–17 (1979).
10. Hata, Y., Tsumoto, T., Sato, H., Hagihara, K. & Tamura, H. *Nature* **335,** 815–817 (1988).
11. Hubel, D. J., Wiesel, T. N. & LeVay, S. *Phil. Trans. R. Soc.* B**278,** 377–409 (1977).
12. Van der Loos, H. & Woolsey, T. A. *Science* **179,** 395–397 (1973).
13. Merzenich, M. M. *et al J. comp. Neurol.* **224,** 591–605 (1984).
14. Stryker, M. P. & Harris, W. A. *J. Neurosci.* **6,** 2117–2133 (1986).
15. Ritter, H. & Schulten, K. *Biol. Cybern.* **54,** 99–106 (1986).
16. Swindale, N. V. *Proc. R. Soc.* B**215,** 211–230 (1982).
17. Hubel, D. J. & Wiesel, T. N. *J. Physiol.* **195,** 215–243 (1968).
18. Wiesel, T. N. & Hubel, D. H. *J. comp. Neurol.* **158,** 307–318 (1974).
19. Linsker, R. *Proc. natn. Acad. Sci. U.S.A.* **83,** 8390–8394 (1986).
20. Miller, K. D., Keller, J. B. & Stryker, M. P. *Science* **245,** 605–615 (1989).

ACKNOWLEDGEMENTS. We thank Nick Swindale and Ken Miller for comments. R.M.D. is a Lucille P. Markey Visiting Fellow, and this work was supported in part by the Lucille P. Markey Charitable Trust.

Calcium/calmodulin-dependent protein kinase II increases glutamate and noradrenaline release from synaptosomes

Robert A. Nichols, Talvinder S. Sihra, Andrew J. Czernik, Angus C. Nairn & Paul Greengard

Laboratory of Molecular and Cellular Neuroscience, The Rockefeller University, New York, New York 10021, USA

A VARIETY of evidence indicates that calcium-dependent protein phosphorylation modulates the release of neurotransmitter from nerve terminals[1–3]. For instance, the injection of rat calcium/calmodulin-dependent protein kinase II (Ca^{2+}/CaM-dependent PK II) into the preterminal digit of the squid giant synapse leads to an increase in the release of a so-far unidentified neurotransmitter induced by presynaptic depolarization[3,4]. But until now, it has not been demonstrated that Ca^{2+}/CaM-dependent PK II can also regulate neurotransmitter release in the vertebrate nervous system. Here we report that the introduction of Ca^{2+}/CaM-dependent PK II, autoactivated[5–8] by thiophosphorylation, into rat brain synaptosomes (isolated nerve terminals) increases the initial rate of induced release of two neurotransmitters, glutamate and noradrenaline. We also show that introduction of a selective peptidergic inhibitor of Ca^{2+}/CaM-dependent PK II inhibits the initial rate of induced glutamate release. These results support the hypothesis[3,9] that activation of Ca^{2+}/CaM-dependent PK II in the nerve terminal removes a constraint on neurotransmitter release.

Because injected Ca^{2+}/CaM-dependent PK II can enhance the release of neurotransmitter at the squid giant synapse[3], we investigated whether a similar phenomenon is observed when the enzyme is introduced into nerve terminals from mammalian brain. To do this, we used a novel freeze–thaw technique that causes a transient permeabilization of rat brain synaptosomes while preserving their viability[10]. To maintain an increased